The Journal of Experimental Medicine

# Transient activation of *c-MYC* expression is critical for efficient platelet generation from human induced pluripotent stem cells

Naoya Takayama,[1] Satoshi Nishimura,[3,4,5] Sou Nakamura,[1] Takafumi Shimizu,[2] Ryoko Ohnishi,[1] Hiroshi Endo,[1,2] Tomoyuki Yamaguchi,[2] Makoto Otsu,[2] Ken Nishimura,[4,6] Mahito Nakanishi,[6] Akira Sawaguchi,[7] Ryozo Nagai,[3,5] Kazutoshi Takahashi,[8] Shinya Yamanaka,[8] Hiromitsu Nakauchi,[2] and Koji Eto[1]

[1]Stem Cell Bank and [2]Division of Stem Cell Therapy, Center for Stem Cell Biology and Regenerative Medicine, the Institute of Medical Science, and [3]Department of Cardiovascular Medicine and [5]Translational Systems Biology and Medicine Initiative, the University of Tokyo, Tokyo 113-0033, Japan
[4]PRESTO, Japan Science and Technology Agency, Tokyo 102-8666, Japan
[6]Gene Function Research Center, National Institute of Advanced Industrial Science and Technology, Ibaraki 305–8562, Japan
[7]Department of Anatomy, University of Miyazaki Faculty of Medicine, Miyazaki 889-1692, Japan
[8]Center for iPS Research and Application, Kyoto University, Kyoto 606-8507, Japan

**Human (h) induced pluripotent stem cells (iPSCs) are a potentially abundant source of blood cells, but how best to select iPSC clones suitable for this purpose from among the many clones that can be simultaneously established from an identical source is not clear. Using an in vitro culture system yielding a hematopoietic niche that concentrates hematopoietic progenitors, we show that the pattern of *c–MYC* reactivation after reprogramming influences platelet generation from hiPSCs. During differentiation, reduction of *c–MYC* expression after initial reactivation of c–MYC expression in selected hiPSC clones was associated with more efficient in vitro generation of CD41a+CD42b+ platelets. This effect was recapitulated in virus integration–free hiPSCs using a doxycycline–controlled c–MYC expression vector. In vivo imaging revealed that these CD42b+ platelets were present in thrombi after laser–induced vessel wall injury. In contrast, sustained and excessive *c–MYC* expression in megakaryocytes was accompanied by increased p14 (*ARF*) and p16 (*INK4A*) expression, decreased *GATA1* expression, and impaired production of functional platelets. These findings suggest that the pattern of *c–MYC* expression, particularly its later decline, is key to producing functional platelets from selected iPSC clones.**

CORRESPONDENCE
K. Eto:
keto@ims.u-tokyo.ac.jp

Abbreviations used: CB, cord blood; DOX, doxycycline; ESC, embryonic stem cell; HDF, human dermal fibroblast; HLA, human leukocyte antigen; iPSC, induced pluripotent stem cell; KO, Kusabira orange; MK, megakaryocyte; PB, peripheral blood; SCF, stem cell factor; Tg, transgene; TPO, thrombopoietin; VEGF-R2, vascular endothelial growth factor type 2 receptor.

Platelets are key elements not only of hemostasis and thrombosis but also of tissue regeneration after injury and the pathophysiology of inflammation (Gawaz et al., 2005; Nesbitt et al., 2009). The production of platelets, thrombopoiesis, is regulated primarily by thrombopoietin (TPO)-mediated megakaryopoiesis within the BM (Patel et al., 2005; Schulze and Shivdasani, 2005). Notably, many patients with critical thrombocytopenia, caused by dysregulation of BM as a result of hematopoietic disease or aggressive chemotherapy, require platelet transfusions using platelet concentrates obtained through blood donation (Webb and Anderson, 1999). It is well known, however, that repeated transfusion induces antibodies in recipients against allogenic human leukocyte antigen (HLA) on the

transfused platelets (Schiffer, 2001). To establish a supply of identical platelet concentrates without loss of responsiveness as a result of immunorejection, particularly for patients with a rare HLA, human (h) induced pluripotent stem cells (iPSCs) represent a potentially abundant source.

Successful reprogramming of differentiated fibroblasts into a pluripotent stage using the defined genes *OCT3/4*, *KLF4*, *SOX2*, and *c-MYC* (Takahashi et al., 2007; Yu et al., 2007) is a potentially effective means of generating HLA-matched iPSCs for regenerative medicine
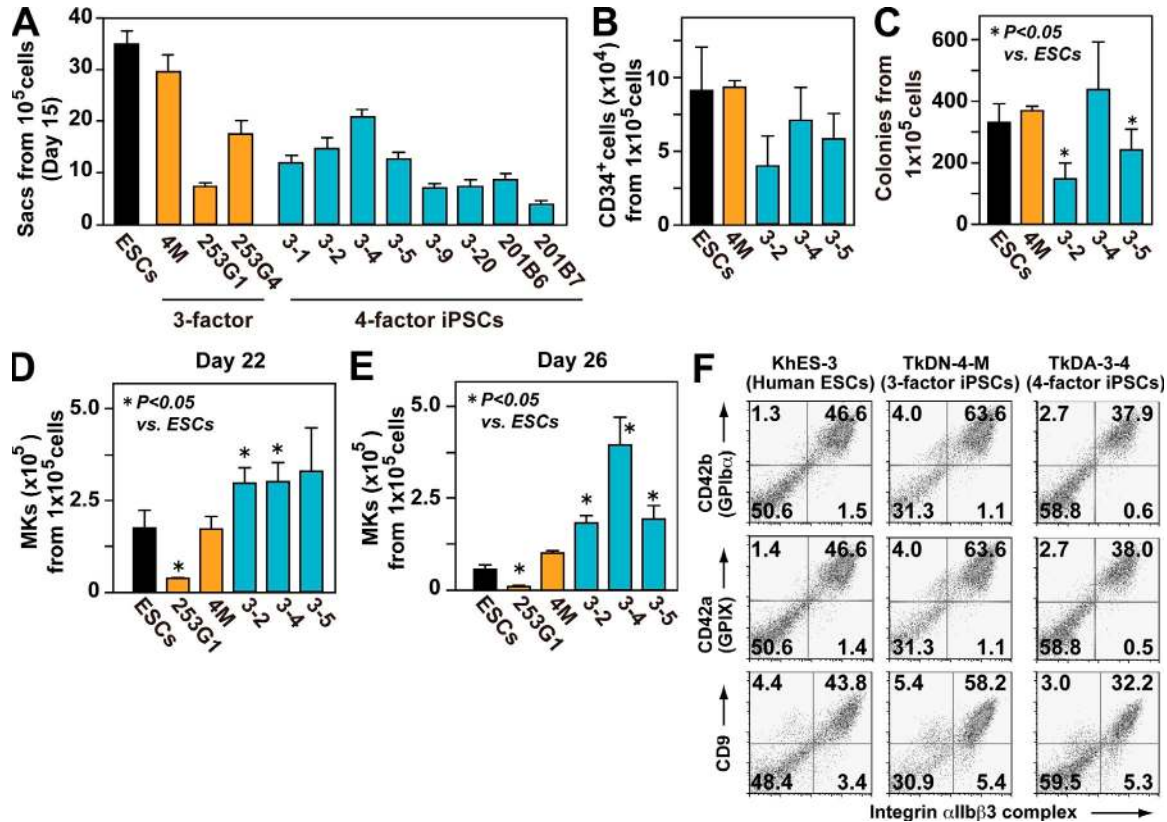
**Figure 1. Four–factor human iPSCs are better than three–factor iPSCs for megakaryopoiesis, which is independent of hematopoietic colony potential.** (A) Numbers of ESC- and iPSC-sac–like structures generated from $10^5$ cells ($n = 3$, means $\pm$ SEM from three independent experiments). (B) Numbers of CD34+ hematopoietic progenitors within ESC- or iPSC-sacs yielded from $10^5$ human ESCs or iPSCs ($n = 3$, means $\pm$ SEM). (C) Numbers of hematopoietic colonies derived from $10^5$ human ESCs or iPSCs within sacs ($n = 3$, means $\pm$ SEM). (D and E) Numbers of CD42b (GPIb$\alpha$)+ MKs derived from $10^5$ hematopoietic progenitors within sacs on day 22 (D) and day 26 (E; $n = 5$, means $\pm$ SEM). (F) Representative flow cytometry dot plots for khES-3–, TkDN-4-M–, and TkDA3-4–derived MKs examined on day 24.

(Raya et al., 2009). However, reactivation of *c-Myc* during establishment of iPSCs can reportedly lead to oncogenicity after transplantation (Okita et al., 2007). But because platelets are anucleate, they can be irradiated before transfusion to eliminate residual hiPSCs or other differentiated nucleated cells that could form teratomas or malignant tumors (van der Meer and Pietersz, 2005). Thus, platelet concentrates derived from hiPSCs could be a useful source of HLA-identical platelets, which eliminates the need for scarce donor blood. That said, because a large number of iPSC clones can be simultaneously generated from an identical source, the iPSC clone most suitable for the desired purpose must be selected before the differentiation phase (Miura et al., 2009). We therefore sought to determine the hallmark of such cells as well as the best way to select iPSC clones in vitro for generation of functional platelets in vivo.

*c-Myc* plays essential roles in both embryonic and adult hematopoiesis, although its effects on megakaryopoiesis and thrombopoiesis in various mouse models remains unclear (Thompson et al., 1996a,b; Chanprasert et al., 2006; Guo et al., 2009). For example, two studies of inducible *c-Myc* overexpression (O/E) under the control of megakaryocyte (MK)-specific differentiation revealed that *c-Myc* plays a positive role

in the proliferation of MK progenitors (Thompson et al., 1996a,b). Moreover, *c-Myc* is reportedly essential for the TPO–c-mpl axis in megakaryopoiesis (Chanprasert et al., 2006). In contrast, recent studies using *c-Myc*–deficient mice showed that the absence of the gene actually led to an increase in the platelet count (Guo et al., 2009).

Using a culture system that yields an in vitro hematopoietic niche containing hematopoietic progenitors (which we named iPS-Sac), we show in this paper that limited reactivation of *c-MYC* and its subsequent decline after a reactivation-dependent increase in the gene's expression in immature MKs are key components of platelet generation in vitro and contribute to the selection and validation of iPSC clones in which genome integration is accomplished through reprogramming. These clones are suitable for transfusion in clinical applications or mechanistic studies of thrombopoiesis using disease-specific iPSCs.

## RESULTS

### Four–factor hiPSC–derived hematopoietic progenitors contribute to enhanced generation of MKs and platelets

Using VSV-G–pseudotyped retroviruses (Ory et al., 1996) harboring human reprogramming factors (*OCT3/4, SOX2,*

2818

c-MYC modulates platelet generation from iPSCs | Takayama et al.

*KLF4*, and/or *c-MYC*), we sought to establish iPSCs from human dermal fibroblasts (HDFs). With our system, we consistently generated 200–300 hiPSC clones from $10^5$ HDFs. For evaluation of pluripotency, established iPSC clones obtained through transduction with four or three factors (with or without *c-MYC*) and all clones showing a normal karyotype (not depicted) were examined for morphology, SSEA-4 expression (Fig. S1 A), other gene expression (Fig. S1 B), and the ability to form teratomas in vivo (Fig. S1 C). Our findings confirmed that exogenous *OCT3/4*, *SOX2*, *KLF4*, and *c-MYC* remained unexpressed in established iPSCs (Fig. S1 B).

To explore the hiPSC clones' potential for differentiation into hematopoietic cells (Takayama et al., 2008), we evaluated several iPS-Sacs (Fig. S2 A) from individual clones (four-factor hiPSCs: TkDA3-1, –2, –4, –5, –9, –20, 201B6, and 201B7; three-factor hiPSCs: TkDN4-M, 253G1, and 253G4) and compared them to previously evaluated human (h) embryonic stem cells (ESCs; KhES3 clone, Kyoto University, Japan; Takayama et al., 2008). On day 15 of culture, iPS-Sacs that contained numerous hematopoietic-like round cells (Fig. S2 B) and showed expression of vascular endothelial growth factor type 2 receptor (VEGF-R2^{+}; Fig. S2 B) or platelet endothelial cell adhesion molecule 1 (CD31^{+}; not depicted) were deemed to be potentially suitable microenvironments from which to obtain hematopoietic progenitors, as was observed in hESC-derived structures (Takayama et al., 2008).

We detected considerable heterogeneity in the production of iPS-Sacs (a hallmark of the efficiency of hematopoietic progenitors) from iPSCs derived from the same source (i.e., TkDA3-1, –2, –4, –5, –9, or –20; Fig. 1 A), which was also consistent with previous observations in hESCs (Osafune et al., 2008). In particular, CD34^{+}, but not CD34^{−}, cells from iPS-Sacs showed successful colony formation in methylcellulose colony assays (Fig. S2 C). The three-factor clone TkDN4-M, as well as KhES-3, appeared to have a greater potential for myeloid lineage hematopoiesis, as exemplified by the numbers of Sacs (Fig. 1 A, red bar) composed of CD34^{+} cells (Fig. 1 B, red bar), and the numbers of hematopoietic colonies formed from each Sac (Fig. 1 C, red bar). Nonetheless, the number of CD42b (GPIbα; von Willebrand factor receptor)[+] MKs obtained with four-factor iPSC clones (e.g., TkDA3-2, TkDA3-4, and TkDA3-5) was higher than that obtained with TkDN4-M or KhES-3 when equal numbers of cells from iPS-Sacs were seeded onto fresh culture dishes in the presence of TPO, stem cell factor (SCF), and heparin (Fig. 1, D [day 22] and E; and Fig. S3 day 26; Takayama et al., 2008). For example, clone TkDA3-4 generated three times as many MKs as TkDN4-M or KhES-3 at the peak of production (Fig. 1 E, day 26; and Fig. S3). By days 22–38, phase-contrast imaging revealed the presence of proplatelets, a prerelease platelet form (Video 1), as well as mature MKs by May-Giemsa staining (Fig. S4). Moreover, flow cytometric analysis showed that 40–60% of floating cells expressed CD41a (integrin αIIbβ3 complex), a fibrinogen receptor, as well as CD42a (GPIX), GPIbα, and CD9, all of which are hallmarks of MKs (Fig. 1 F; Tomer, 2004; Takayama et al., 2008).
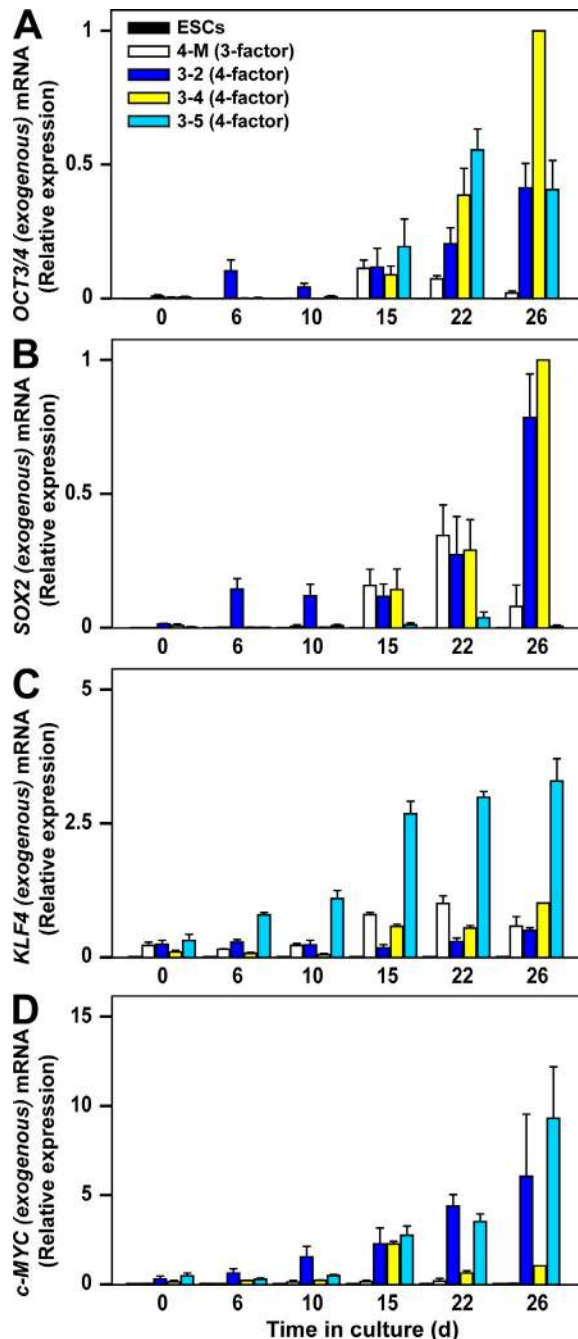


**Figure 2. Time-dependent changes in qPCR induced by exogenous reprogramming genes in three-factor or four-factor iPSCs.** mRNA encoding exogenous *OCT3/4* (A), *SOX2* (B), *KLF4* (C), and *c-MYC* (D) in human ES cells (ESCs), TkDN4-M (three-factor iPSCs), TkDA3-2, TkDA3-4, and TkDA3-5 (four-factor iPSCs) on day 0 or their derivatives (on days 6, 10, 15, 22, and 26 after initiation of MK-lineage culture) were examined by qPCR as described in the Materials and methods section. TkDA3-4–derived mature MKs (day 26) was assigned a value of 1.0 ($n = 4$, means ± SEM from two independent experiments).

To determine the mechanism underlying the enhanced megakaryopoiesis exhibited by four-factor hiPSC–derived hematopoietic progenitors, we assessed the potential of progenitors
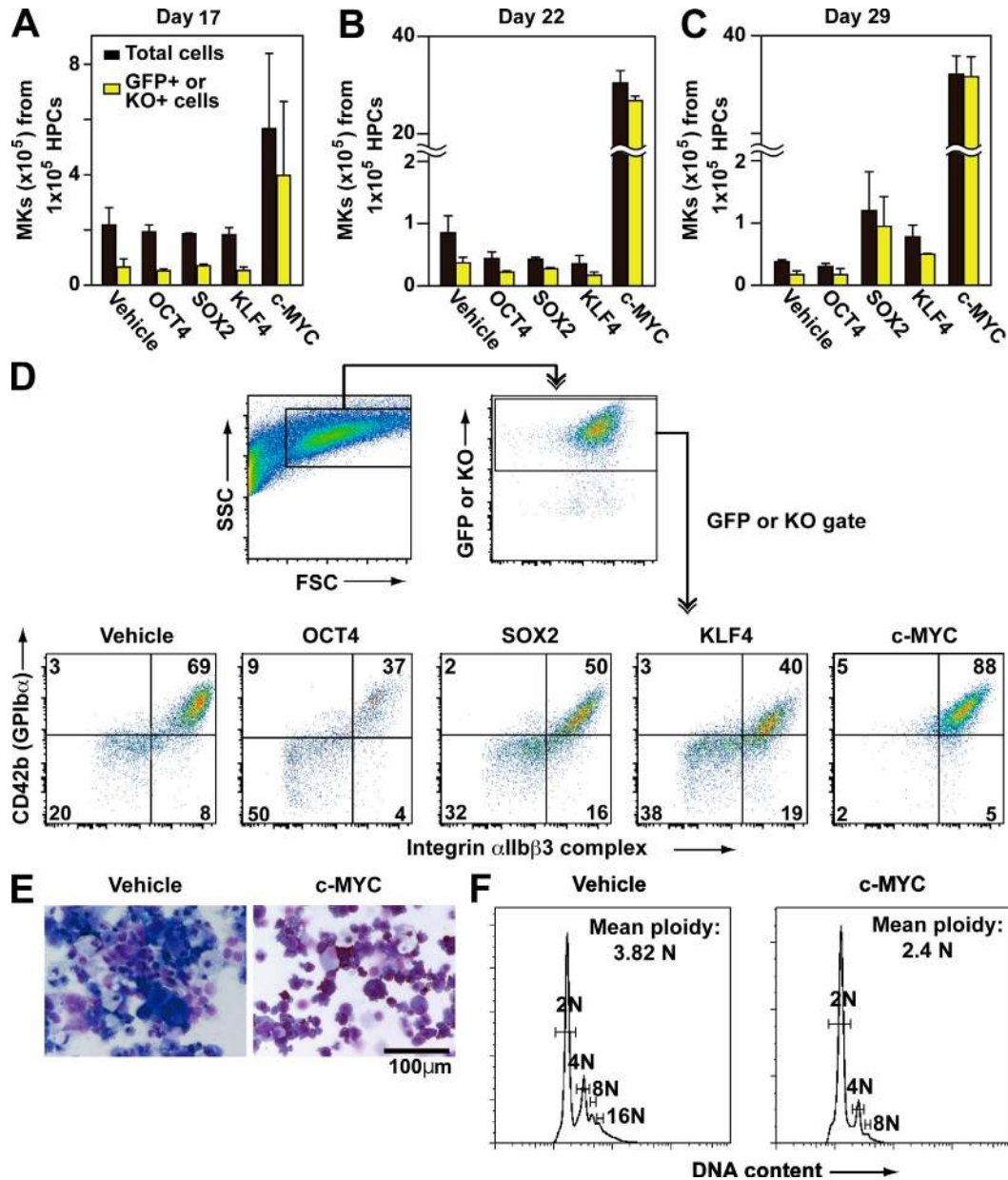
**Figure 3. Effects of reprogramming factors on megakaryopoiesis.** (A–C) Each reprogramming factor was transduced, together with EGFP or KO markers, on day 15 of MK-lineage culture. Numbers of total and marker genes EGFP or KO-expressing cells in floating cells on day 17 (A) and CD42b+ MKs on days 22 (B) and 26 (C) were measured (*n* = 3, means ± SEM). (D) Representative flow cytometry dot plots of hESC-derived hematopoietic cells transduced with vehicle (EGFP), *OCT3/4-KO*, *SOX2-EGFP*, *KLF4-EGFP*, or *c-MYC-EGFP* on day 22. (E and F) On day 22, May-Giemsa staining (E) or ploidy analysis (F) of the cells transduced with vehicle or *c-MYC* was examined.

within iPS-Sacs, based on colony-forming capacity (Fig. S2 D) and their surface markers (not depicted). We found no significant differences between TkDA3-4 (four-factor) and TkDN4-M (three-factor; Fig. S2 D), which means the potential and the capacity to drive most myeloid lineage commitment from iPSC-derived progenitors is independent of the clone type, or at least there was no detectable difference between the three- and four-factor iPSC clones we examined (not depicted).

In contrast, quantitative (q) PCR analysis of hematopoietic cells on days 22–26 (7–11 d after replating for selective

MK lineage culture) revealed expression of the exogenous (transgene [Tg]) reprogramming genes, which were not expressed before hematopoiesis (Fig. 2, A–D, day 0; and Fig. S1 B). Although qPCR after day 15 suggested that, in four-factor iPSCs, activation of *OCT3/4* Tg and/or *c-MYC* Tg might affect the enhanced megakaryopoiesis (Fig. 2, A and D), individual Tg activation was not dependent on the copy number in the genome (Fig. S1, D and E).

Thus, to confirm the functional effect of *OCT3/4* and/or *c-MYC* Tg on megakaryopoiesis from pluripotent stem cells,
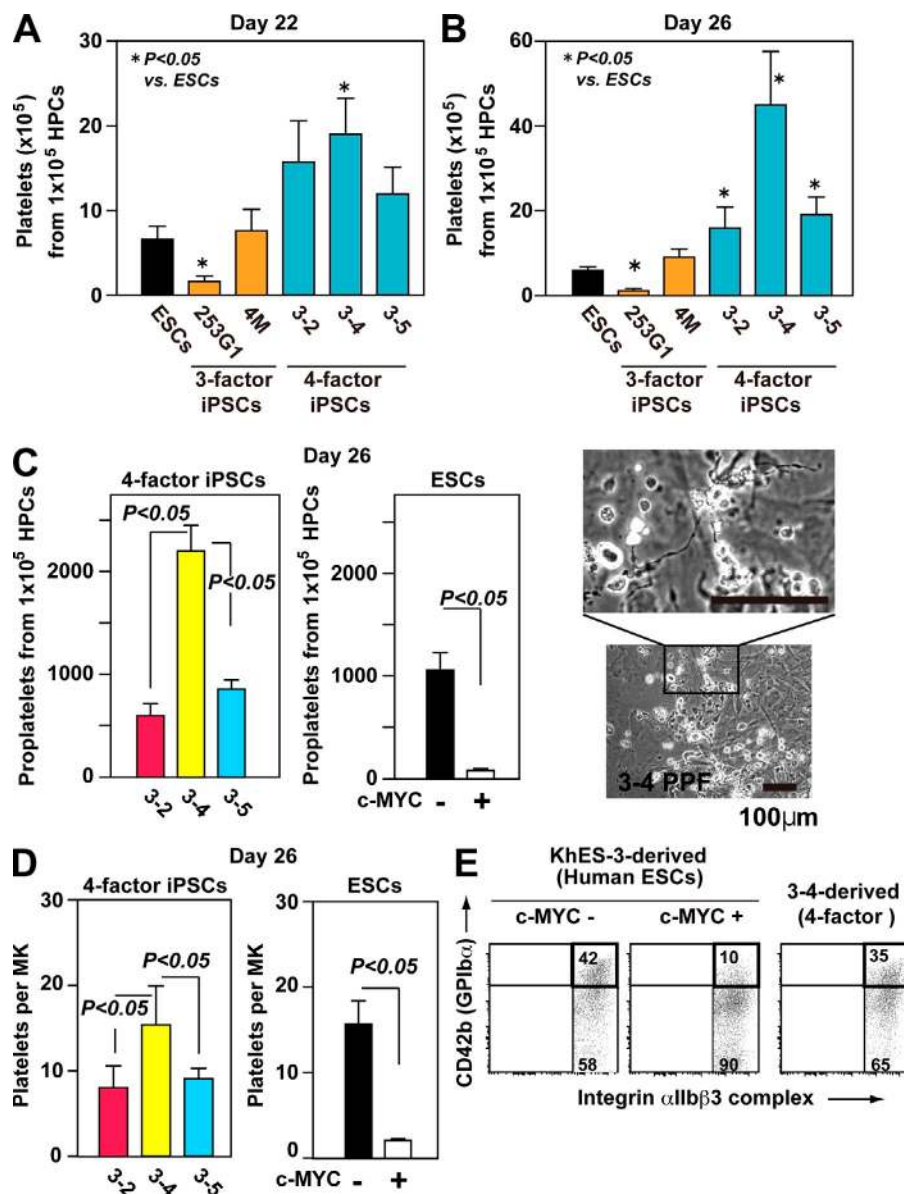
Figure 4. Level of *c–MYC* reactivation in individual iPSC–derived MKs may determine the efficiency of platelet generation in vitro. (A and B) Numbers of CD41a+CD42b+ platelets generated from hESCs or hiPSCs on days 22 (A) and 26 (B; peak of platelet generation; n = 5, means ± SEM). (C and D) Numbers of proplatelets (C) and platelets (D) derived from four-factor iPSCs and from ESC hematopoietic progenitors, with or without *c–MYC* transduction (ii; n = 5, means ± SEM). Representative photomicrographs of proplatelets are derived from four-factor iPSCs. (D) Numbers of platelets per MK was calculated as the total number of platelets divided by the total number of MKs on day 26 (n = 5, means ± SEM). (E) Representative flow cytometry dot plots show MKs derived from TkDA3-4 and KhES-3, with or without c-MYC transduction, on day 26.

## *c–MYC* levels in hiPSC–derived MKs determines the number of platelets generated per MK

We next tested whether iPSC–derived MKs actually yield platelets in vitro. We confirmed that four-factor iPSCs generate greater numbers of platelets than three-factor iPSCs or hESCs (Fig. 4, A and B; and Fig. S5). Moreover, we noticed that, at the peak of production (day 26), many more proplatelets and platelets were generated from TkDA3-4 iPSCs than from any other four-factor iPSCs (Fig. 4, B and C; and Fig. S5). We also noted that TkDA3-2 and TkDA3-5 iPSC-derived MKs showed an earlier peak, on day 22 (Fig. 1, D and E; and Fig. S3) and that there were

each reprogramming factor was separately introduced into hematopoietic progenitors derived from KhES-3, along with EGFP or Kusabira orange (KO), which served as markers. Only *c-MYC* expression recapitulated the time course of the enhanced megakaryopoiesis, as it was accompanied by greater transduction efficiency as a result of the increased cell proliferation it induced (Fig. 3, A–C). Flow cytometry revealed that on day 22, most of the EGFP+ or KO+ population was CD41a+CD42b+ in the *c-MYC* O/E specimens but not in the others (Fig. 3 D), although only mononuclear and lower ploidy cells were present (Fig. 3, E and F). These suggest that *OCT3/4* O/E might not accelerate megakaryopoiesis (Fig. 3 D). Collectively then, these findings suggest that stronger expression of *c-MYC* in hESCs might promote lineage commitment into megakaryopoiesis without maturation.

fewer proplatelets in the dishes (Fig. 4 C), which suggests that most MKs promote apoptosis and/or senescence leading to inhibition of platelet release in those two clones.

It has been reported that forced expression of *c-Myc* impairs maturation of MKs displaying polyploidization, leading to an increase in immature MKs (Thompson et al., 1996a). Indeed, we confirmed the appearance of immature MKs (Fig. 3, D–F) on day 22 after retroviral transduction of *c-MYC* into hESC-derived hematopoietic progenitors, which diminished proplatelet formation and platelet yield (Fig. 4, C and D; and Fig. S6 A). Dot plots for CD41a+CD42b+ platelets obtained by flow cytometric analysis of KhES-3, TkDN4-M (three-factor iPSCs), and TkDA3-4 (four-factor iPSCs) showed similar patterns (Fig. 4 E and Fig. S6 A), although most of the CD41a+CD42b− platelets appeared to have shed the extracellular domain of
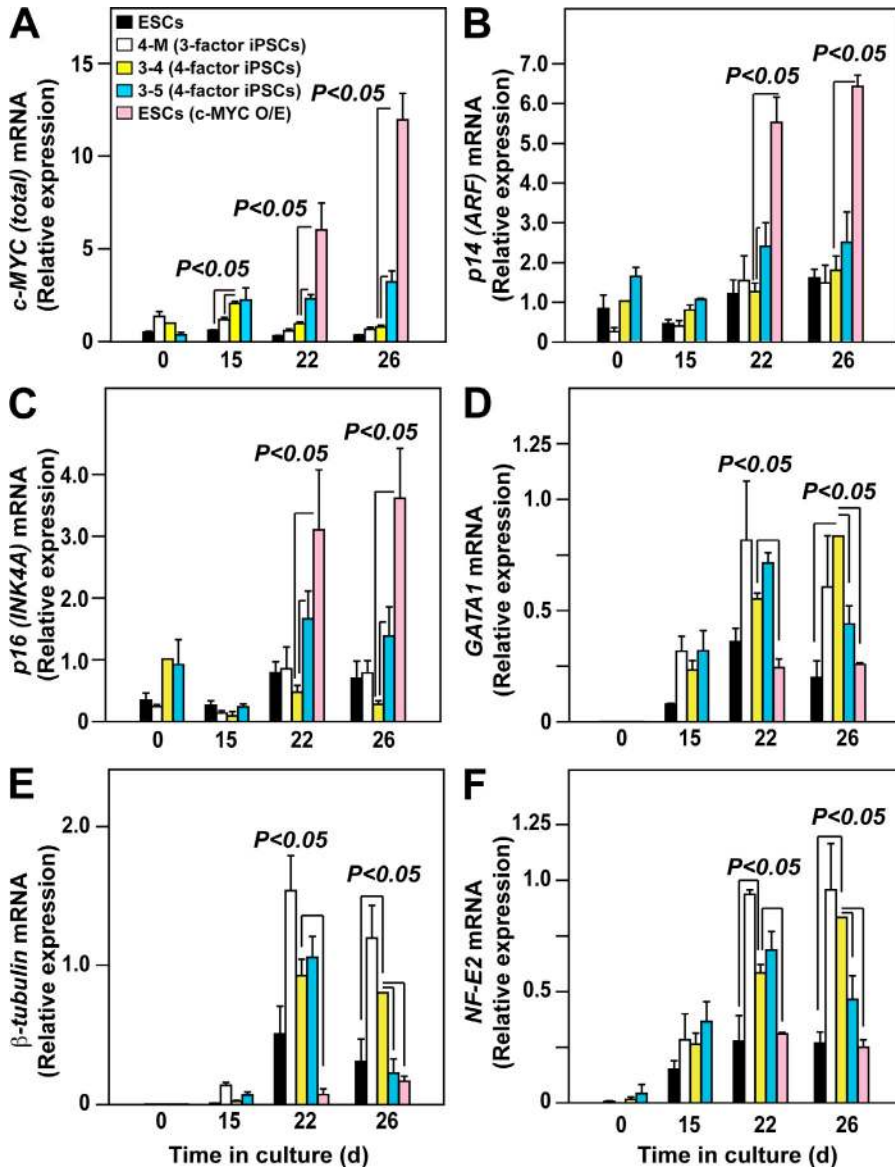
**Figure 5. Level of *c-MYC* expression affects INK4A/ARF locus genes and genes related to MK maturation during mega-karyopoiesis from pluripotent stem cells.** qRT-PCR analysis of total *c-MYC* (A, endogenous plus exogenous), *p14ARF* (B), *p16INK4A* (C), *GATA1* (D), *β1-tubulin* (E), and *NF-E2 p45* (F) expression in hESCs, with and without overexpression (O/E) of exogenous *c-MYC*, on days 22 and 26 (7 and 11 d after transduction) in three-factor hiPSCs (TkDN4-M) or in four-factor hiPSCs (TkDA3-4 and TkDA3-5) on days 0, 15, 22, and 26. All levels were normalized to the level of *GAPDH* expression ($n = 4$ of two independent samples). The levels of *c-MYC* (A), *p14ARF* (B), *and p16INK4A* (C) expression in an undifferentiated TkDA3-4 iPSC clone (day 0) or expression of the other genes (D–F) in TkDA3-4–derived mature MKs (day 26) was assigned a value of 1.0 ($n = 4$, means ± SEM).

*c-MYC* and the genes involved in *c-MYC* activation and thrombopoiesis. qPCR analyses confirmed that total (endogenous plus exogenous) *c-MYC* expression in TkDA3-4, TkDA3-5, and *c-MYC*-O/E hESCs (KhES-3) was higher than in TkDN4-M (three-factor) or hESCs without *c-MYC* (control) on days 15 (hematopoietic progenitors) and 22 (immature MKs) of culture (Fig. 5 A). Intriguingly, however, total *c-MYC* expression in TkDA3-5 increased progressively from days 15 through 26, whereas in TkDA3-4, the iPSC clone showing the most efficient platelet generation, total *c-MYC* expression declined after day 15

CD42b (GPIbα), as indicated by the recovery of CD42b expression in the presence of a metalloprotease inhibitor (Fig. S6 B; Nishikii et al., 2008). In contrast, platelet-like particles from hESC-derived MKs ectopically expressing *c-MYC* (*c-MYC*-O/E) showed significantly lower CD42b expression, a distinct pattern on dot plots (Fig. 4 E and Fig. S6 A), and no recovery of CD42b expression after administration of metalloprotease inhibitor (not depicted). Given the platelet generation per MK, it appears that forced expression of *c-MYC* in ESCs impairs platelet yield on day 26 (Fig. 4 D), which might recapitulate in TkDA3-2 or TkDA3-5 iPSC-MKs (Fig. 4 D).

## How does the level of *c-MYC* expression control platelet generation from iPSCs?

The results so far suggest that excess *c-MYC* expression diminishes platelet yield. To confirm that hypothesis, we evaluated the time-dependent changes in the total expression of

(Fig. 5 A). To confirm whether reactivation actually influenced total c-MYC expression (Fig. 5 A), we separately examined endogenous and exogenous (Tg) *c-MYC* expression. We found that although levels of total and exogenous *c-MYC* differed among the clones (Fig. 5 A and Fig. S7 A), there was no significant difference in endogenous c-MYC levels among TkDN4-M, TkDA3-4, and TkDA3-5 (Fig. S7 B). In contrast, expression of two INK4A locus genes, *p14* (*ARF*) and *p16* (*INK4A*), which act as a safety net system against *c-Myc* hyper-activation leading to senescence (Murphy et al., 2008), was higher in *c-MYC*-O/E hESCs and TkDA3-5 than in TkDA3-4 on day 22 (immature MKs; Fig. 5, B and C). We therefore assumed that elevation of *p14* and *p16*, beginning at an earlier phase of differentiation, is associated with inhibition of MK maturation (Fig. 3, E and F). MYC associates with the GATA1 promoter during immature erythroblast expansion, perhaps suppressing GATA-1 expression (Rylski et al., 2003). Similarly,
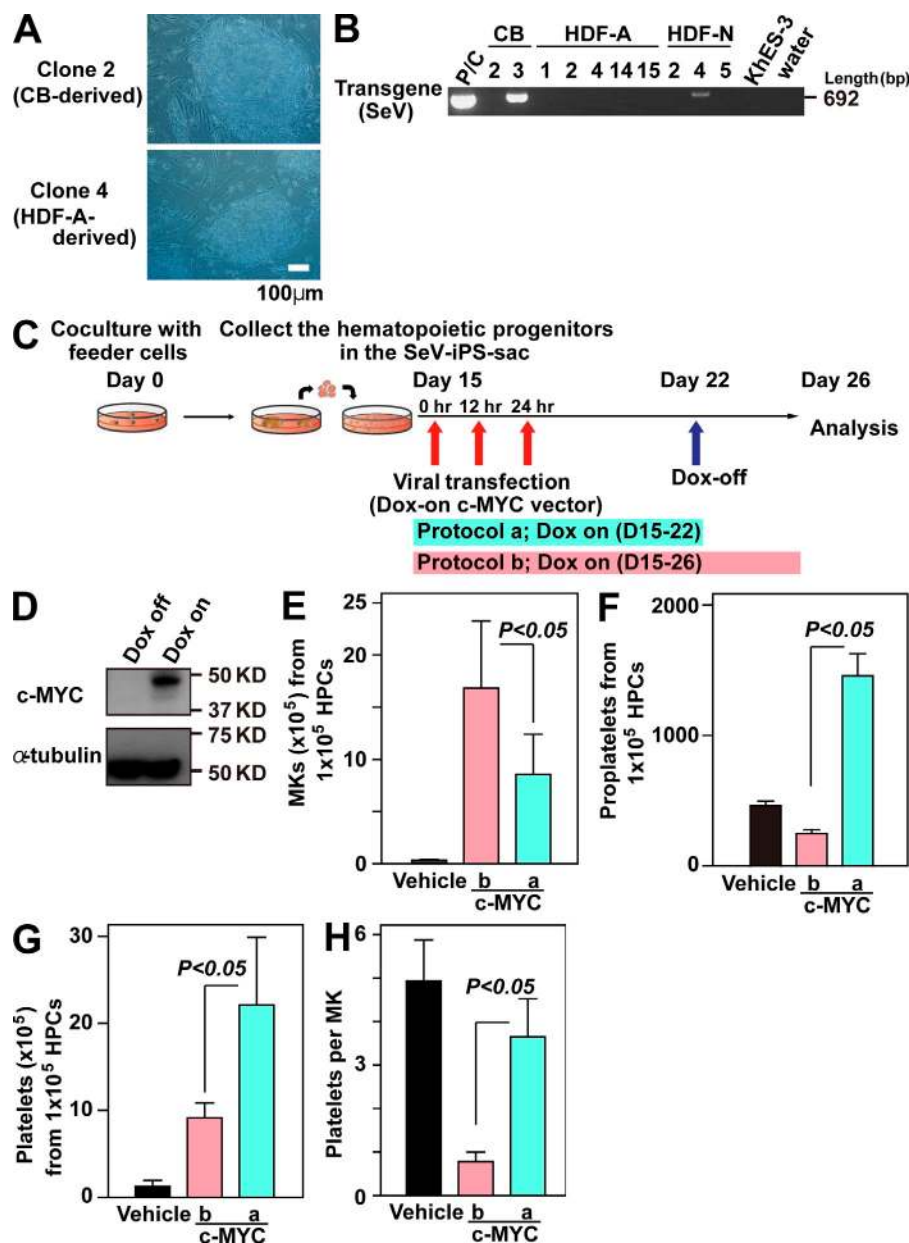
**Figure 6. Inducible c-MYC expression system enabling Sendai viral vector–based iPSCs without reactivation to recapitulate enhanced MK maturation with increased platelet generation.** (A) Representative photomicrographs of SeV-iPSCs derived from CB CD34+CD45+ cells or HDFs. Original magnification, 100×. (B) RT-PCR analyses of Sendai virus Tg (harboring reprogramming factors) expression in SeV-iPSC clones (passage number 4) derived from CB, HDF-A (adult), and HDF-N (neonate). A sample of HDFs transduced with SeV is used as a positive control for the SeV Tg. (C) Scheme of *c-MYC* induction in SeV-iPSC–derived hematopoietic cells. Hematopoietic progenitors derived from SeV-iPSCs were transfected with DOX-inducible *c-MYC* O/E vector on day 15 and analyzed on day 26. In Protocol a, DOX was added only from days 15 to 22. In protocol b, DOX was added from days 15 through 26. (D) Representative Western blots of cell lysates with *c-MYC* O/E (DOX-on; protocol b) or without *c-MYC* O/E (DOX-off; Protocol a) on day 26. The α-tubulin levels indicate same protein value. (E–G) Numbers of CD42b (GPIbα)+ MKs (E), proplatelets (F), and platelets (G) on day 26 derived from $10^5$ hematopoietic progenitors transfected with vehicle or DOX-inducible c-MYC O/E vector in protocol a or protocol b ($n = 4$, means ± SEM). (H) Numbers of platelets per MK generated on day 26 of culture (peak of platelet generation; $n = 4$, means ± SEM). Numbers of platelets per MK were calculated as the total number of platelets divided by the total number of MKs on day 26.

*GATA-1* expression was reduced in *c-MYC*-O/E hESC (KhES-3)-MKs showing higher levels of *c-MYC* expression on day 22, as were levels of *β1-tublin* and *NF-E2* (*p45*; Fig. 5, D–F). Consistent with those findings, both *c-MYC*-O/E MKs and TkDA3-5–derived MKs showed less proplatelet formation (Fig. 4 C) and had a smaller platelet yield than TkDA3-4 (Fig. 4 D). Thus, high levels of sustained expression of *INK4A* locus genes in MKs are also associated with impaired platelet release.

These results suggest that an increase in *c-MYC* expression, peaking on day 22, followed by a decline may be critical for efficient platelet generation on day 26, as exemplified in TkDA3-4. Sustained increases in *c-MYC* expression may contribute to activation of senescence genes, thereby impairing MK maturation and intact platelet yield.

## Inducible *c-MYC* expression in iPSCs without reactivation exhibited behavior similar to that of iPSCs with reactivation, leading to efficient generation of functional platelets

To further confirm whether an increase and subsequent decline in c-MYC is critical for megakaryopoiesis, leading to an efficient platelet yield, we prepared a Sendai viral vector (SeV) harboring the four reprogramming genes, which, during the generation of human iPSCs, enabled RNA viral transduction without integration of DNA into the chromosome (Nishimura et al., 2007; Fig. 6, A and B). Thereafter, doxycycline (DOX)–inducible expression system in a lentiviral vector was applied to the SeV-based human iPSCs (SeV-iPSCs; skin-fibroblast [HDF]-derived SeV-iPSCs and cord blood [CB] CD34+ cell–derived SeV-iPSCs; Fig. 6 A). We selected CB-derived SeV-iPSCs (clone 2; Fig. 6, A and B) for most experiments because they showed no detectable Tg and better differentiation to hematopoietic progenitors than other clones, including HDF-derived SeV-iPSCs (not depicted). *c-MYC* O/E was regulated by DOX (Fig. 6 C), and
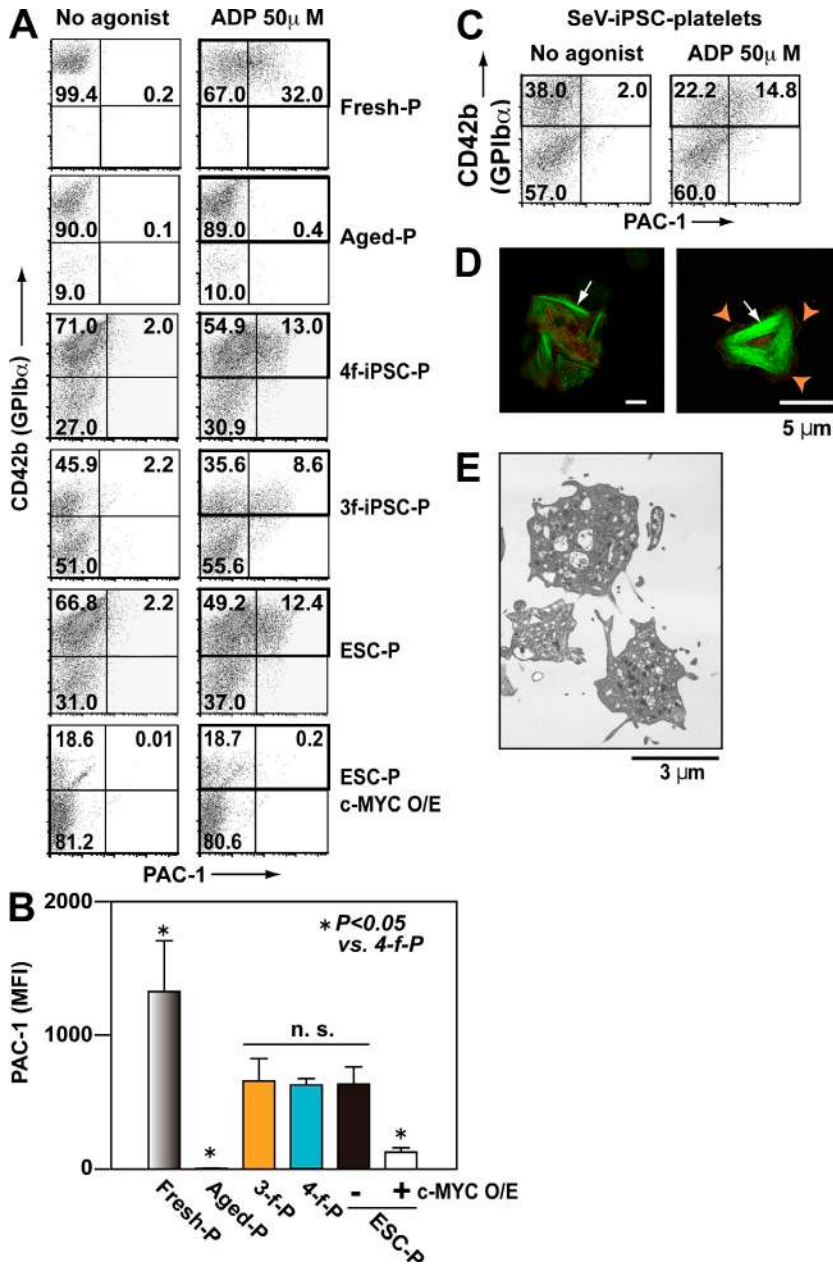
**A** No agonist | ADP 50μ M

Fresh-P: 99.4 | 0.2 | 67.0 | 32.0
Aged-P: 90.0 | 0.1 | 89.0 | 0.4 — 9.0 | 10.0
4f-iPSC-P: 71.0 | 2.0 | 54.9 | 13.0 — 27.0 | 30.9
3f-iPSC-P: 45.9 | 2.2 | 35.6 | 8.6 — 51.0 | 55.6
ESC-P: 66.8 | 2.2 | 49.2 | 12.4 — 31.0 | 37.0
ESC-P c-MYC O/E: 18.6 | 0.01 | 18.7 | 0.2 — 81.2 | 80.6

CD42b (GPIbα) ; PAC-1 →

**C** SeV-iPSC-platelets

No agonist | ADP 50μ M

38.0 | 2.0 | 22.2 | 14.8
57.0 | 60.0

CD42b (GPIbα) ; PAC-1 →

**D** 5 μm

**E** 3 μm

**B** PAC-1 (MFI) ; *P<0.05 vs. 4-f-P ; n. s.

Fresh-P, Aged-P, 3-f-P, 4-f-P, − + c-MYC O/E (ESC-P)

**Figure 7. Integrin activation and the structure of human iPSC platelets are comparable to those in human PB–derived platelets.** (A–C) Integrin activation in fresh human platelets (Fresh-P), aged human platelets (48-h incubation at 37°C; Aged-P), TkDN4-M (three-factor iPSC) platelets (3f-iPSC-P), TkDA3-4 (four-factor iPSC) platelets (4f-iPSC-P), and ESC platelets (ESC-P), with or without *c-MYC* O/E. The binding of PAC-1 (indicative of platelet activation) to individual platelets was quantified in the absence and presence of 50 μM ADP using flow cytometry. (A) Representative flow cytometry dot plots. Square indicates CD42b+ platelets. (B) Mean fluorescence intensity (MFI) of bound PAC-1, obtained from square gate in A. Error bars depict means ± SEM for four independent experiments (duplicate). (C) Representative flow cytometry analysis of PAC-1–bound platelets generated from integration-free SeV-iPSCs subjected to biphasic activation and, thereafter, decline of c-MYC expression as protocol b shown in Fig. 6 C. Square indicates CD42b+ platelets. (D) Spreading of iPSC platelets on fibrinogen. Human CD41a (red) and phalloidin (green) were used to identify F-actin fibers. Arrowheads indicate lamellipodia. Arrows indicate actin stress fibers. Bars, 5 μm. (E) Transmission electron micrographs of hiPSC (TkDA3-4) platelets on day 26. Bar, 3 μm.

integrin activation in human platelets (from peripheral blood [PB]), PB-based aged platelets (48-h incubation; Bergmeier et al., 2003; Nishikii et al., 2008), iPSC platelets, and ESC platelets. The aged platelets were tested because iPSC–derived platelets were heterogeneously produced from MKs at various stages in culture, so that many of the platelets produced could have become aged (Nishikii et al., 2008). Conformational changes in integrins are required for platelet aggregation and stable thrombosis in vivo (Shattil et al., 1985). Indeed, although PB-based aged platelets were nonresponders, the integrin activity of TkDA3-4 (four-factor iPSCs) platelets was comparable to that of TkDN4-M (three-factor iPSCs) platelets, which showed a weaker response than human PB platelets (Fig. 7, A and B; and Fig. S8 A). Notably, *c-MYC* O/E-dependent iPSC-derived platelets showed little binding (Fig. 7, A and B). In contrast, platelets produced from SeV-iPSCs-MKs in the absence of *c-MYC* O/E after its activation responded well to ADP stimulation (Fig. 7 C). We therefore conclude that *c-MYC* activation and decline during MK differentiation may lead to the generation of functional platelets from iPSCs. We also examined expression of P-selectin (CD62P) on platelets in the presence of 50 μM ADP and observed weak but positive P-selectin expression in iPSC-derived platelets (Fig. S8 B).

we confirmed that day 22 was the most suitable point to turn off O/E. The results also showed that continuous *c-MYC* O/E from days 22 to 26 still increased the number of MKs (Fig. 6 E), whereas the lack of *c-MYC* O/E from days 22 to 26 increased the total numbers of proplatelets (Fig. 6 F) or CD41a+CD42b+ platelets (Fig. 6 G). An increase in platelet yield per MK was also evident with the absence of *c-MYC* O/E after day 22 (Fig. 6 H), confirming the effect of *c-MYC* expression on megakaryopoiesis.

### Human iPSC–derived platelets function normally in vitro and in vivo

To assess the effect of *c-MYC* reactivation on the functionality of platelets from TkDA3-4, we compared agonist-induced
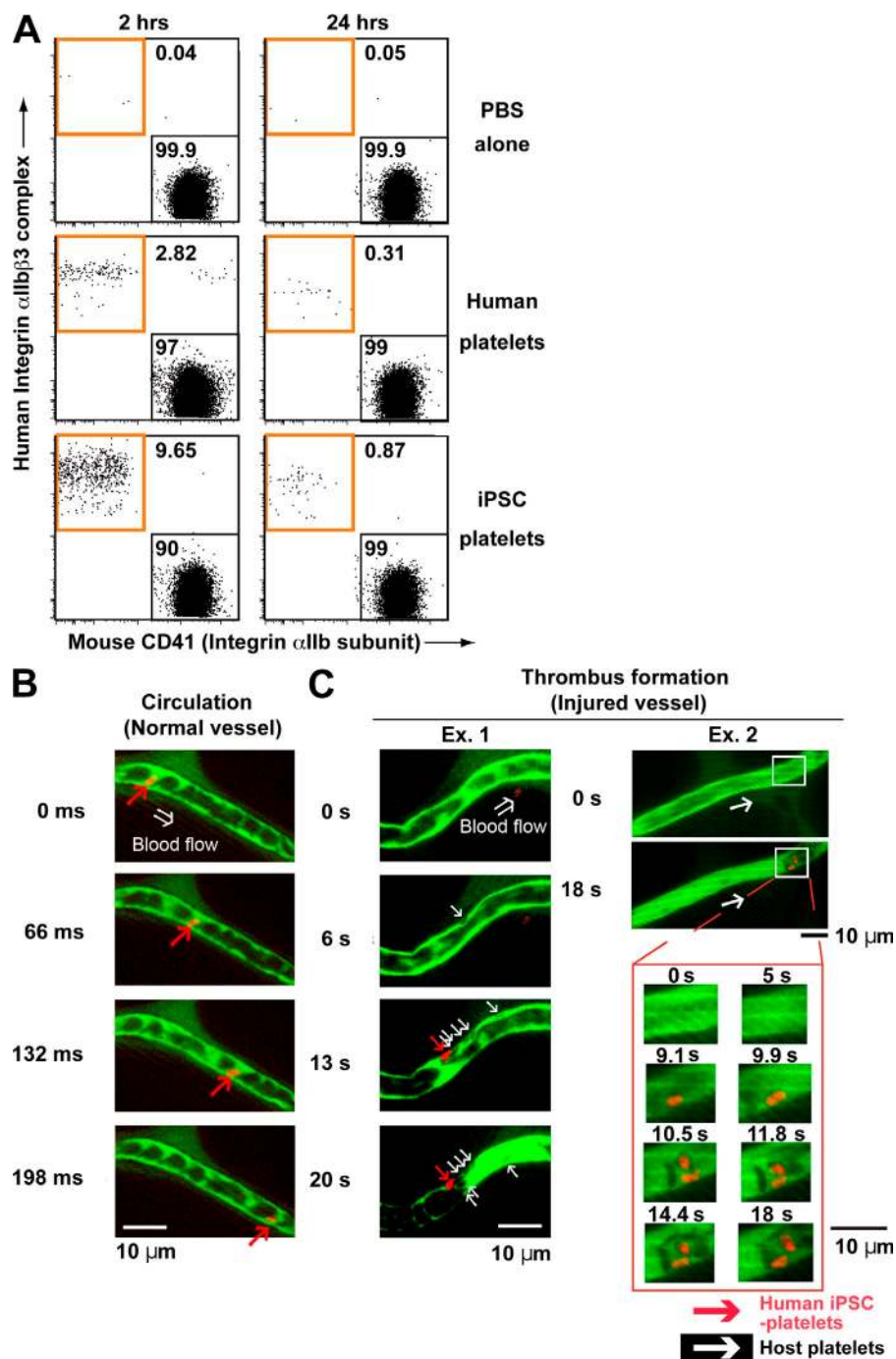
**Figure 8. Human iPSC platelets circulate in NOG mice and adhere to vessel during thrombus formation in vivo.** (A) NOG (nod-scid/IL-2 γc-null) mice were irradiated (2.0 Gy) to induce thrombocytopenia. 9 d later, human iPSC platelets, human PB-derived platelets (10⁷), or PBS alone was injected via the tail vein. Platelet chimerism was quantified by flow cytometry. Representative dot plots for the same experiment are shown. Circulation of injected platelets was evaluated after 2 and 24 h (orange squares). Experiments were independently performed three times. (B) Sequential images of circulating iPSC platelets. A combination of FITC-dextran (green) and 10⁷ TMRE-stained iPSC platelets (red) in PBS was injected via the tail vein into NOG mice. Mesenteric capillaries were visualized using a confocal laser-scanning microscope. Red arrows indicate circulating iPSC platelets in vivo. Original videos are available as Video 2. (C) Representative sequential images of thrombus formation by iPSC platelets in a blood vessel. Hematoporphyrin was administrated to induce thrombus formation after laser-induced injury, as described previously (Nishimura et al., 2008; Takizawa et al., 2010). Red arrows indicate iPSC platelets in a developing thrombus. White arrows indicate host (mouse) platelets. Original videos are available as Videos 3–5. Experiments were independently performed three times. Bars, 10 μm.

TkDA3-4 iPSC platelets on immobilized fibrinogen exhibited filopodia, lamellipodia, and/or actin stress fibers, all of which are also indicative of platelet thrombosis (Shattil et al., 1985; Fig. 7 D), suggesting that appropriate elevation and then reduction of *c-MYC* expression increases production efficiency without impairing platelet functionality, at least in vitro. Moreover, the granule content and structural components of TkDA3-4 iPSC platelets appeared normal when examined under transmission electron microscopy (Fig. 7 E), which implies a capacity for hemostasis in vivo.

In contrast, as in the previous paragraph, we recently showed that culture at 37°C influences the degradation of platelets by causing them to shed the extracellular domain of GPIbα, which is required for initial adhesion to the injured vessel wall (Nishikii et al., 2008; Fig. S6 B). In vivo, platelets lacking the GPIbα extracellular domain are quickly cleared from the circulation (Bergmeier et al., 2003), leading to insufficient levels of circulating platelets after transfusion (Nishikii et al., 2008). To avoid this without affecting platelet yield, we applied GM6001, a nonspecific inhibitor to metalloproteases, for 2 d before collection of cultured platelets and confirmed that the shedding of GPIbα was dose-dependently inhibited by GM6001 (Fig. S6 B; Nishikii et al., 2008).

We next sought to develop a transfusion model to assess platelet circulation in vivo. Using a NOG (nod-scid/IL-2 γc-null) mouse thrombocytopenia model induced by irradiation (2.0 Gy, 9 d beforehand), flow cytometric analyses performed

2 and 24 h after transfusion ($\sim$1.0–1.2 × 10$^7$ platelets/mouse) showed that four-factor iPSC platelets were consistently present and that the percentage circulating was similar to that obtained with fresh human platelets (platelet chimerism of human CD41a$^+$/mouse CD41a$^+$; 3–10%, 2 h after transfusion; Fig. 8 A).

To further assess and confirm the functionality of TkDA3-4 hiPSC platelets in vivo, we used the same NOG mouse model (Fig. 8 A) with high–spatiotemporal resolution confocal laser microscopy to visualize the behavior of individual platelets upon initiation of adhesion to an injured vessel wall and during the subsequent steps in thrombus formation under flow within the vessel (Takizawa et al., 2010). iPSC platelets stained with tetramethylrhodamine ethyl ester, which is incorporated into the external lipid layer of the cell membrane, were transfused into NOG mice (2 Gy, 14 d beforehand), after which we confirmed they circulated as individual platelets (Fig. 8 B, red; and Video 2). Then using our novel laser injury thrombus model (Takizawa et al., 2010), we clearly observed that iPSC platelets initially adhered to the injured vessel wall, coordinating with host platelets and ultimately leading to thrombus formation and vessel occlusion (Fig. 8 C; and Videos 3–5). Thus, four-factor iPSC platelets appear capable of mediating hemostasis and thrombosis in vivo.

## DISCUSSION

Megakaryocytic lineage–restricted *c-Myc* expression in mouse models showed this gene to be a positive regulator of MK progenitor proliferation (Thompson et al., 1996a,b) and to be required for TPO/c-mpl signaling in megakaryopoiesis (Chanprasert et al., 2006). Notably, *c-Myc* deficiency also accelerates megakaryopoiesis, but with lower ploidy (up to 8n), and augments immature platelet release accompanied by an increase in the platelet count. In our hiPSC culture system, however, total cellular *c-MYC* expression (endogenous plus reactivation of exogenous) appeared to be at an appropriate, and probably restricted, level suitable for promoting platelet generation (Fig. 4 B, Fig. 5 A, and Fig. 6 G, day 26). Increasing MYC levels enables cells to move from quiescence to S phase, even in the absence of mitogens (Eilers et al., 1991), possibly through activation of target genes (*cyclin D1(D2,D3)/Cdk4(6)* and *cyclin E/Cdk2*). In that regard, although MYC activity, per se, is required for normal cell proliferation (Murphy et al., 2008), it is recognized that above a certain threshold *c-Myc* expression may induce the onset of oncogenesis. Moreover, excessively high MYC levels induce senescence via activation of the Arf–Mdm2–p53 pathway (Eischen et al., 1999; Murphy et al., 2008) and suppression of key regulators of MK maturation, such as GATA1, β1-tubulin, and NFE2, which likely inhibits maturation (Fig. 5, B–F) and may also induce apoptosis in some cells (Askew et al., 1991; Evan et al., 1992).

Four-factor hiPSC-derived hematopoietic progenitors also generate much larger numbers of platelets than three-factor iPSCs or hESCs (Fig. 4, A and B; and Fig. S5), possibly as a result of MK proliferation mediated though *c-MYC* reactivation (Fig. 3 A; Fig. 4, A and B; and Fig. S3). However, the

number of platelets per MK derived from individual four-factor hiPSC clones (TkDA3-2, -4, and -5; with *c-MYC*) and ESCs (with or without *c-MYC*) on day 26 differs (Fig. 4 D). Nonetheless, TkDA3-4, which is the most efficient platelet-producing clone (Fig. 4, B and D; and Fig. S5), shows weaker *c-MYC* expression than other four-factor iPSCs or *c-MYC*-O/E MKs (Fig. 5 A). Indeed, DOX–inducible expression of *c-MYC* O/E in genome integration-free iPSCs (SeV-iPSCs) confirmed our hypothesis (Fig. 6, A–H). In addition, when we considered the possibility that deregulated MK maturation leads to release of nonfunctional platelets, we found differences in platelet functionality between hESCs or SeV-iPSCs, with or without *c-MYC*, and iPSC clones (Fig. 7, A–C). Immature megakaryocytic cell lines, such as Meg01, are reportedly capable of releasing CD41a$^+$ platelet–like particles, but they show poor functionality in vitro (Takeuchi et al., 1998). We also found that hESC-derived CD41$^+$ particles showed significantly less CD42b expression when *c-MYC* was ectopically expressed in MKs (Fig. 4 E and Fig. S6 A) and showed poor functionality in vitro (Fig. 7, A and B). In contrast, the function of CD42b$^+$ platelets generated from TkDA3-4 was intact and able to mediate hemostasis in vivo, although some of the yield was likely made up of nonfunctional aged platelets (Fig. 7 and Fig. 8 C).

To clarify the underlying mechanism, we examined the association between platelet generation and gene expression. In *c-MYC*-O/E MKs, expression of *GATA1* (Vyas et al., 1999; Rylski et al., 2003), a key regulator for MK maturation and polyploidization, was suppressed, whereas *INK4A* and *ARF* expression was greatly up-regulated (Fig. 5, B–D; Eischen et al., 1999; Murphy et al., 2008). Consequently, the maturation phase was inhibited, as exemplified by the presence of hypoploid cells without proplatelets (Fig. 3, E and F; and Fig. 4 C) and the weak expression of mature MK markers β1-tubulin and *NF-E2* (Fig. 5, E and F), as well as *platelet factor 4* (not depicted; Patel et al., 2005; Schulze and Shivdasani, 2005). These MKs only generated a few nonfunctional CD41a$^+$CD42b$^+$ platelets (Fig. 4, D and E; Fig. 5 A; and Fig. 7 B). In contrast, MKs derived from TkDA3-4 transiently showed appropriately high levels of *c-MYC* expression, with no effect on expression of *INK4A/ARF* locus genes (Fig. 5, A [day 15], B, and C), after which *c-MYC* expression declined (Fig. 5 A, days 22 and 26). From days 22 to 26, the pattern of *GATA1*, β1-tubulin, and *NF-E2* expression was opposite that of *c-MYC* expression (Fig. 5, D–F), indicating that reduction of *c-MYC* after day 22 (immature MKs) may be required for MK maturation and generation of functional platelets (e.g., day 26). We therefore suppose that because most MKs derived from TkDA3-5, which produced fewer platelets than TkDA3-4 (Fig. 4 D), showed sustained *c-MYC* activity, leading to up-regulation of *INK4A/ARF* locus genes (Fig. 5), those MKs were unable to complete the maturation phase, even though *GATA-1*, β1-tubulin, and *NF-E2* expression was enhanced (Fig. 5, D–F). We further confirmed this phenomenon using integration-free SeV-iPSCs in a DOX-inducible gene expression system. Removal of *c-MYC* O/E from day 22 until day 26 increased the total numbers of proplatelets (Fig. 6 F) and

CD42b$^+$ functional platelets (Fig. 6 G and Fig. 7 C), as compared with the numbers seen with continuous $c$-MYC O/E until day 26. We therefore conclude that increased expression of $c$-MYC in hematopoietic progenitors may promote megakaryopoiesis, leading to increased MK generation (Fig. 6 E), but that a sustained increase in $c$-MYC after the MK progenitor stage may impair MK maturation, thereby diminishing platelet release (Fig. 6, F and G).

Both hESCs and hiPSCs were previously shown to differentiate into hematopoietic cells (Wang et al., 2004; Vodyanik et al., 2005; Ma et al., 2008; Choi et al., 2009; Yokoyama et al., 2009), although with the exception of hESC-derived natural killer cells (Woll et al., 2009), only in vitro functionality has been reported. In this paper, we demonstrated that platelets derived from hiPSCs via a mechanism involving limited $c$-MYC reactivation (Fig. 4 B and Fig. 5 A) are capable of thrombus formation in vivo.

Recent studies suggest that the source of the somatic cells and introduction of reprogramming factors without $c$-$Myc$ (retroviral vectors, plasmids, proteins, Sendai viral vectors, and so on), also known as $L$-$Myc/L$-$MYC$, are essential elements for selection of efficient and safe iPSC clones (Okita et al., 2007; Nakagawa et al., 2010). We propose that selection of the iPSC clones most suitable for their purpose should also be considered. Our analysis of multiple hiPSC clones accompanied by Tg genome integration or a DOX-inducible expression system shows that time-dependent changes in $c$-MYC expression, specifically up-regulation and then down-regulation within an appropriate time span, facilitates generation of a novel platelet transfusion system derived from hiPSCs. It is noteworthy that in vitro generation of platelet concentrates custom made from HLA-identical donors or the patients themselves are not subject to immune rejection and do not require donor blood. We propose that iPSC platelets could be an invaluable resource for patients requiring repeated platelet transfusion and that this system should enable us to investigate as yet unresolved aspects of the mechanisms underlying thrombocytopenia.

## MATERIALS AND METHODS

**Cells, reagents, viral vectors, and mice.** All reagents were obtained from Sigma-Aldrich unless indicated otherwise. The human ESC clone Kyoto hESCs (KhES) 3 was obtained from the Institute for Frontier Medical Science, Kyoto University (Kyoto, Japan) after approval for hESC use was granted by the Minister of Education, Culture, Sports, Science, and Technology of Japan. PB was provided from healthy volunteers approved by ethical committee of the Institute of Medical Science at University of Tokyo for human sample-based experiments. The entire study using human samples was conducted in accordance with the Declaration of Helsinki. Animal experiments and use of viral vectors were approved by the committees of the Institute of Medical Science and School of Medicine at University of Tokyo. pMX retroviral vectors were from T. Kitamura (The University of Tokyo, Tokyo, Japan). Original hiPSC clones, 201B6, 201B7, 253G1, and 253G4 (Kyoto University), were used as a reference (Takahashi et al., 2007). We established other hiPSC clones derived from HDFs (Cell Applications, Inc.) using a retrovirus harboring four ($OCT3/4$, $SOX2$, $KLF4$, and $c$-MYC) or three (without $c$-MYC) reprogramming factors: TkDA3-1, -2, -4, -5, -9, and -20 and TkDN4-M clones. HDFs were cultivated in DME supplemented with 10% FBS, 2 mM L-glutamine, 100 U/ml penicillin, and 0.1 mg/ml streptomycin. All pluripotent cells were maintained as described previously (Takahashi et al., 2007).

The mouse C3H10T1/2 cell line was purchased from the Institute of Physical and Chemical Research Bio-Resource Center (Tsukuba, Ibaraki, Japan) and was cultured as described previously (Takayama et al., 2008). Retroviral supernatants for establishing iPSCs were obtained from a 293 GPG system (provided by R.C. Mulligan, Children's Hospital Boston, Boston, MA; Ory et al., 1996). SeV vector harboring human $OCT3/4$, $SOX2$, $KLF4$, and $c$-MYC was based upon original SeV vector and viral supernatants were made as previously described (Nishimura et al., 2007). Another set of hiPSCs without genome integration was established using SeV harboring four factors from HDFs or CB CD34$^+$/CD45$^+$ cells (Lonza). Hematopoietic differentiation from iPSCs and hESCs was performed in the same medium, as described previously (Takayama et al., 2008). The following antibodies were used: PE-conjugated anti-CD9, PE-conjugated anti-CD31, PE- or FITC-conjugated anti-CD34, unconjugated or allophycocyanin (APC)-conjugated anti-CD41a (HIP8 clone), FITC-conjugated anti-CD42a, PE-conjugated anti-CD42b, Alexa Fluor 405–conjugated anti-CD45, and APC-conjugated anti–VEGF-R2. FITC-conjugated PAC-1 (BD) and FITC-conjugated anti-CD62P (P-selectin; BioLegend) antibodies were used for platelet activation studies (Shattil et al., 1985). Tirofiban (Takayama et al., 2008), a specific antagonist of human integrin αIIbβ3, was obtained from Merck. Anti–c-Myc (1:400; Santa Cruz Biotechnology, Inc.), anti–α-tubulin (1:1,000; Sigma-Aldrich), anti–mouse IgG-HRP (1:5,000; GE Healthcare), and anti–rabbit IgG-HRP (1:2,500; GE Healthcare) antibodies were used for Western blotting. 15-wk-old NOG mice were obtained from the Central Institute for Experimental Animals (Kanagawa, Japan) and were maintained under specific pathogen-free conditions. The mice were irradiated at 2.0 Gy to induce thrombocytopenia and have analyzed for platelet chimerism using an Aria flow cytometer (BD) or by in vivo imaging using a confocal laser-scanning microscope (CSU-X1; Yokogawa Electronics).

**Induction of human iPSCs using high-titer retroviruses or SeV viruses.** hiPSCs were established from HDFs using high-titer retroviruses derived from 293GPG cells (Ory et al., 1996). Integration-free human iPSCs were established with SeV harboring human $OCT3/4$, $SOX2$, $KLF4$, and $c$-MYC as described in the previous section. CB cells were infected with SeV in the same basal medium (Takayama et al., 2008) supplemented with 50 ng/ml human SCF (R&D Systems), human TPO (R&D Systems), and human FMS–related tyrosine kinase 3 ligand (FLT3-L; PeproTech).

**Immunohistochemistry of human ESCs and human iPSCs.** hiPSCs were fixed with 4% paraformaldehyde in PBS, after which they were labeled first with an antibody against human SSEA4 (Millipore) and then with a secondary antibody and observed using an epifluorescence microscope (DM IRBE; Leica).

**Semi-qRT-PCR.** hiPSCs were lysed with Trizol (Invitrogen), after which total RNA was extracted as recommended by the manufacturer. Complementary DNAs were obtained using an RT-PCR System (Thermo Fisher Scientific) and oligo-dT primers (Invitrogen). Samples were normalized to intrinsic $GAPDH$. Semi-qRT-PCR was performed to determine the expression levels of genes of interest. Amplification proceeded for 26–32 cycles. The primer sets used are shown in Table S1.

**Teratoma formation and histological analysis.** hiPSCs were prepared from 10$^7$ cells/ml in PBS. Male NOD/Scid mice were anesthetized with diethyl ether, after which aliquots of suspended cells (1–3 × 10$^6$ cells) were injected into their testes. 8 wk after injection, the mice were sacrificed, and the resultant tumors were dissected. Tumor samples were then fixed in 4% paraformaldehyde, embedded in paraffin, sectioned, and stained with hematoxylin and eosin.

**Southern blotting analysis.** 7 μg of genomic DNA was digested with BglII, EcoRI, and NcoI or NaeI, NdeI, and NcoI for c-MYC or Oct3/4, respectively, overnight. Digested DNA fragments were separated on 0.8% agarose gel and transferred to a nylon membrane (GE Healthcare). The membranes were

hybridized with radioactively labeled DNA probes (c-MYC-exon3 or Oct3/4-exon1) in PerfectHyb Plus Hybridization buffer (Sigma-Aldrich) at 55°C overnight with constant agitation. After washing, signals were detected by the FLA-5100 imaging system (Fujifilm).

**Hematopoietic differentiation of hiPSCs.** To differentiate hiPSCs into hematopoietic cells, we used the same protocol we established with hESCs (Takayama et al., 2008). In brief, small clumps of hiPSCs (<100 cells treated with PBS containing 0.25% trypsin, 1 mM CaCl₂, and 20% KSR) were transferred onto irradiated C3H10T1/2 cells and co-cultured in hematopoietic cell differentiation medium, which was refreshed every 3 d. On days 14–15 of culture, the iPS-Sacs were collected into a 50-ml tube, gently crushed with a pipette and passed through a 40-μm cell strainer to obtain hematopoietic progenitors, which were transferred onto freshly irradiated feeder cells and cultured in differentiation medium established as previously in human ESCs (Takayama et al., 2008). The medium was refreshed every 3 d, and nonadherent cells were collected and analyzed from days 22 to 38.

**DOX-inducible c-MYC lentiviral vector.** The *c-MYC* gene-inducible lentiviral vector was based upon LV-TRE-mOKS-Ubc-tTA-I2G (Kobayashi et al., 2010) and made by replacing the mOKS cassette with *c-MYC* gene. Viral supernatant was generated as previously described (Eto et al., 2007).

**Western blotting analysis.** Experiments were performed as previously described (Eto et al., 2007; Nishikii et al., 2008). In brief, 45 μg of cell lysates treated with TNE buffer (10 mM Tris-HCl, pH 7.8, 150 mM NaCl, 1% NP-40, and 1 mM EDTA), supplemented with protease inhibitor cocktail (Roche), were separated by electrophoresis on 10–20% SDS–polyacrylamide gradient gel (Bio-Rad Laboratories) and transferred to a polyvinylidine difluoride membrane (Millipore), followed by visualization with SuperSignal West Pico Chemiluminescent Substrate (Thermo Fisher Scientific).

**Immunohistochemical and flow cytometric analyses of ES- and iPS-Sacs.** Immunohistochemical staining of iPS-Sacs was performed on day 14 or 15. Intact iPS-Sacs were fixed with 10% methanol in PBS, after which they were stained first with an antibody against human VEGF-R2 and then with a secondary antibody and observed using an epifluorescence microscope (DM IRBE; Leica). Round cells within the ES- and iPS-Sacs were stained with anti–human CD31-PE, CD34-FITC, CD38-APC, CD41a-APC, CD45–Alexa Fluor 405, or VEGF-R2–APC antibodies and analyzed by flow cytometry.

**Hematopoietic colony-forming cell assay.** Hematopoietic colony-forming cell assays were performed in MethoCult H4434 semisolid medium (STEMCELL Technologies Inc.) supplemented with 50 ng/ml human TPO. 10,000 hematopoietic progenitors from within an iPS-Sac were plated in 1.5 ml of medium and cultivated for 14 d. The colonies were then collected, stained with Hemacolor (Merck), and observed under a microscope.

**Flow cytometric analysis of MKs.** Nonadherent cells on days 22–38 were prepared in PBS containing 2% FBS and stained with combinations of antibodies for 30 min on ice. Samples were then washed with PBS and analyzed by flow cytometry (FACSAria; BD).

**Viral transduction of hematopoietic progenitors within ES-sacs.** A total of $10^5$ hematopoietic progenitors harvested from within an ES-sac or iPS-sac on day 15 of culture were suspended in hematopoietic differentiation medium containing 50 ng/ml of human SCF, 100 ng/ml of human TPO, 25 U/ml heparin, and 10 mg/ml protamine sulfate and then transduced with viral supernatant for vehicle, *OCT3/4-KO*, *SOX2-EGFP*, *KLF4-EGFP*, *c-MYC-EGFP*, or DOX-inducible *c-MYC*. The cells were then replated into a 6-well plate precoated with C3H10T1/2 cells and centrifuged at 900 rpm for 60 min at 32°C. The viral transduction was performed three times with 12-h intervals in between. To induce *c-MYC* O/E, 1 μg/ml DOX was added to the culture medium from days 15 to 22 or 26 (Fig. 5 C).

**qRT-PCR.** cDNA samples were prepared as described in the previous section. Real-time PCR was performed using a kit (TaqMan Gene Expression Master Mix [Applied Biosystems] or SYBR Premix Dimer Eraser [Takara Bio, Inc.]) according to the manufacturer's instructions. Signals were detected using an ABI7900HT Real-Time PCR System (Applied Biosystems). Primer sets for *GAPDH*, *c-MYC*, *p14ARF*, *p16INK4A*, *GATA-1*, *β1-tubulin*, and *NF-E2 p45* were determined using the Universal Probe Library Set for humans (https://www.roche-applied-science.com/sis/rtpcr/upl/index.jsp?id=UP030000). Primer sets for exogenous OCT3/4, SOX2, KLF4, c-MYC, and endogenous c-MYC are listed in Table S1.

**Electron microscopic observation of hiPSC-derived platelets.** Platelet pellets were fixed with a mixture of 0.5% glutaraldehyde and 2% paraformaldehyde in 0.1 M phosphate buffer, pH 7.4, for 60 min at 4°C. After washing with phosphate buffer, the samples were post-fixed with 1% osmium tetroxide in phosphate buffer for 60 min on ice. After dehydration, samples on coverslips were infiltrated with and embedded in Epoxy resin. Ultrathin sections (60–80 nm thick) were cut and stained with 2% uranyl acetate in 70% methanol and Reynolds' lead citrate and observed in a transmission electron microscope (1200EX; JEOL) operating at 80 kV.

**Flow cytometric analysis of platelets.** Washed platelets were prepared as described previously (Takayama et al., 2008). The resultant platelet pellets were resuspended with PBS and stained with anti–human CD41a (integrin αIIb/β3 complex)-APC, GPIX-FITC, GPIbα, or CD9-PE for 30 min at room temperature. The platelets were then diluted in 200 μl PBS and analyzed by flow cytometry. Platelet numbers were estimated using true count beads (BD).

**In vitro functional analysis of platelets derived from human iPSCs.** Collected platelets were resuspended in an appropriate volume of modified Tyrode-Hepes buffer (10 mM Hepes, pH 7.4, 12 mM NaHCO₃, 138 mM NaCl, 5.5 mM glucose, 2.9 mM KCl, and 1 mM MgCl₂) and eventually used after addition of 1 mM CaCl₂. To investigate integrin αIIbβ3 activation, 50-μl aliquots of fresh PB- or PB-based aged, hESC-, and hiPSC-derived platelets (ESC platelets and iPSC platelets) were incubated with PE-conjugated anti-GPIbα and FITC-conjugated PAC-1 (Shattil et al., 1985) or FITC-conjugated CD62P (P-selectin) in the absence or presence of human thrombin or ADP for 20 min at room temperature. The binding of PAC-1 to platelets was quantified using an Aria flow cytometer. Nonspecific binding was determined in the presence of 10 μM tirofiban, a specific antagonist of human integrin αIIbβ3 (Peerlinck et al., 1993). Specific binding was defined as total minus nonspecific binding.

**In vivo imaging by iPSC-platelets.** Details of this method are provided elsewhere (Nishimura et al., 2008; Takizawa et al., 2010). In brief, to visually analyze iPSC platelet function, including circulation and thrombus formation in the mesentery of living animals, mice were anesthetized and a small incision was made in the abdominal wall. Intravital imaging was then performed through this small (∼3 mm) window. FITC-dextran (20 mg/kg body weight) was injected into the tail vein for visualization of host blood cell dynamics. iPSC-derived platelets were stained with 5 μM TMRE for 15 min, washed, and injected into the mice. To induce thrombus formation, hematoporphyrin (1.8 mg/kg body weight) was also administrated. Sequential two-color images were obtained for 20 s at 30 frames/s using a high-speed spinning-disk confocal laser scanning microscope (CSU-X1) and a pair of EM charge-coupled device cameras (iXon). All experiments were approved by the University of Tokyo Ethics Committee for Animal Experiments and strictly adhered to the guidelines for animal experiments of the University of Tokyo.

**Statistical analysis.** All data are presented as the mean ± SEM. We used two-tailed Student's *t* tests for statistical analysis; values of P < 0.05 were considered significant.

**Online supplemental material.** Fig. S1 depicts the character of hiPSCs derived from HDFs. Fig. S2 shows the generation of hematopoietic progenitors

from hiPSCs. Figs. S3 and S4 show the time courses of MK generation. Fig. S5 shows the time course of platelet generation. Fig. S6 depicts the representative dot plots of PB-derived and hiPSC-derived platelets. Fig. S7 describes the time-dependent change of exogenous and endogenous c-MYC expression in hESCs and hiPSCs. Fig. S8 shows the in vitro functionality of iPSC platelets. Video 1 shows a typical proplatelet formation. Video 2 demonstrates in vivo imaging of circulating iPSC platelets. Videos 3–5 demonstrate in vivo imaging of iPSC platelet or platelets in thrombi by laser-induced vessel wall injury. Table S1 is a list of primers used in this study. Online supplemental material is available at http://www.jem.org/cgi/content/full/jem.20100844/DC1.

## REFERENCES

Askew, D.S., R.A. Ashmun, B.C. Simmons, and J.L. Cleveland. 1991. Constitutive c-myc expression in an IL-3-dependent myeloid cell line suppresses cell cycle arrest and accelerates apoptosis. *Oncogene*. 6:1915–1922.

Bergmeier, W., P.C. Burger, C.L. Piffath, K.M. Hoffmeister, J.H. Hartwig, B. Nieswandt, and D.D. Wagner. 2003. Metalloproteinase inhibitors improve the recovery and hemostatic function of in vitro-aged or –injured mouse platelets. *Blood*. 102:4229–4235. doi:10.1182/blood-2003-04-1305

Chanprasert, S., A.E. Geddis, C. Barroga, N.E. Fox, and K. Kaushansky. 2006. Thrombopoietin (TPO) induces c-myc expression through a PI3K- and MAPK-dependent pathway that is not mediated by Akt, PKCzeta or mTOR in TPO-dependent cell lines and primary megakaryocytes. *Cell. Signal*. 18:1212–1218. doi:10.1016/j.cellsig.2005.09.010

Choi, K.D., J. Yu, K. Smuga-Otto, G. Salvagiotto, W. Rehrauer, M. Vodyanik, J. Thomson, and I. Slukvin. 2009. Hematopoietic and endothelial differentiation of human induced pluripotent stem cells. *Stem Cells*. 27:559–567.

Eilers, M., S. Schirm, and J.M. Bishop. 1991. The MYC protein activates transcription of the alpha-prothymosin gene. *EMBO J*. 10:133–141.

Eischen, C.M., J.D. Weber, M.F. Roussel, C.J. Sherr, and J.L. Cleveland. 1999. Disruption of the ARF-Mdm2-p53 tumor suppressor pathway in Myc-induced lymphomagenesis. *Genes Dev*. 13:2658–2669. doi:10.1101/gad.13.20.2658

Eto, K., H. Nishikii, T. Ogaeri, S. Suetsugu, A. Kamiya, T. Kobayashi, D. Yamazaki, A. Oda, T. Takenawa, and H. Nakauchi. 2007. The WAVE2/Abi1 complex differentially regulates megakaryocyte development and spreading: implications for platelet biogenesis and spreading machinery. *Blood*. 110:3637–3647. doi:10.1182/blood-2007-04-085860

Evan, G.I., A.H. Wyllie, C.S. Gilbert, T.D. Littlewood, H. Land, M. Brooks, C.M. Waters, L.Z. Penn, and D.C. Hancock. 1992. Induction of apoptosis in fibroblasts by c-myc protein. *Cell*. 69:119–128. doi:10.1016/0092-8674(92)90123-T

Gawaz, M., H. Langer, and A.E. May. 2005. Platelets in inflammation and atherogenesis. *J. Clin. Invest*. 115:3378–3384. doi:10.1172/JCI27196

Guo, Y., C. Niu, P. Breslin, M. Tang, S. Zhang, W. Wei, A.R. Kini, G.P. Paner, S. Alkan, S.W. Morris, et al. 2009. c-Myc-mediated control of cell fate in megakaryocyte-erythrocyte progenitors. *Blood*. 114:2097–2106. doi:10.1182/blood-2009-01-197947

Kobayashi, T., T. Yamaguchi, S. Hamanaka, M. Kato-Itoh, Y. Yamazaki, M. Ibata, H. Sato, Y.S. Lee, J. Usui, A.S. Knisely, et al. 2010. Generation of rat pancreas in mouse by interspecific blastocyst injection of pluripotent stem cells. *Cell*. 142:787–799. doi:10.1016/j.cell.2010.07.039

Ma, F., Y. Ebihara, K. Umeda, H. Sakai, S. Hanada, H. Zhang, Y. Zaike, E. Tsuchida, T. Nakahata, H. Nakauchi, and K. Tsuji. 2008. Generation of functional erythrocytes from human embryonic stem cell–derived definitive hematopoiesis. *Proc. Natl. Acad. Sci. USA*. 105:13087–13092. doi:10.1073/pnas.0802220105

Miura, K., Y. Okada, T. Aoi, A. Okada, K. Takahashi, K. Okita, M. Nakagawa, M. Koyanagi, K. Tanabe, M. Ohnuki, et al. 2009. Variation in the safety of induced pluripotent stem cell lines. *Nat. Biotechnol*. 27:743–745. doi:10.1038/nbt.1554

Murphy, D.J., M.R. Junttila, L. Pouyet, A. Karnezis, K. Shchors, D.A. Bui, L. Brown-Swigart, L. Johnson, and G.I. Evan. 2008. Distinct thresholds govern Myc's biological output in vivo. *Cancer Cell*. 14:447–457. doi:10.1016/j.ccr.2008.10.018

Nakagawa, M., N. Takizawa, M. Narita, T. Ichisaka, and S. Yamanaka. 2010. Promotion of direct reprogramming by transformation-deficient Myc. *Proc. Natl. Acad. Sci. USA*. 107:14152–14157. doi:10.1073/pnas.1009374107

Nesbitt, W.S., E. Westein, F.J. Tovar-Lopez, E. Tolouei, A. Mitchell, J. Fu, J. Carberry, A. Fouras, and S.P. Jackson. 2009. A shear gradient-dependent platelet aggregation mechanism drives thrombus formation. *Nat. Med*. 15:665–673. doi:10.1038/nm.1955

Nishikii, H., K. Eto, N. Tamura, K. Hattori, B. Heissig, T. Kanaji, A. Sawaguchi, S. Goto, J. Ware, and H. Nakauchi. 2008. Metalloproteinase regulation improves in vitro generation of efficacious platelets from mouse embryonic stem cells. *J. Exp. Med*. 205:1917–1927. doi:10.1084/jem.20071482

Nishimura, K., H. Segawa, T. Goto, M. Morishita, A. Masago, H. Takahashi, Y. Ohmiya, T. Sakaguchi, M. Asada, T. Imamura, et al. 2007. Persistent and stable gene expression by a cytoplasmic RNA replicon based on a noncytopathic variant Sendai virus. *J. Biol. Chem*. 282:27383–27391. doi:10.1074/jbc.M702028200

Nishimura, S., I. Manabe, M. Nagasaki, K. Seo, H. Yamashita, Y. Hosoya, M. Ohsugi, K. Tobe, T. Kadowaki, R. Nagai, and S. Sugiura. 2008. In vivo imaging in mice reveals local cell dynamics and inflammation in obese adipose tissue. *J. Clin. Invest*. 118:710–721.

Okita, K., T. Ichisaka, and S. Yamanaka. 2007. Generation of germline-competent induced pluripotent stem cells. *Nature*. 448:313–317. doi:10.1038/nature05934

Ory, D.S., B.A. Neugeboren, and R.C. Mulligan. 1996. A stable human-derived packaging cell line for production of high titer retrovirus/vesicular stomatitis virus G pseudotypes. *Proc. Natl. Acad. Sci. USA*. 93:11400–11406. doi:10.1073/pnas.93.21.11400

Osafune, K., L. Caron, M. Borowiak, R.J. Martinez, C.S. Fitz-Gerald, Y. Sato, C.A. Cowan, K.R. Chien, and D.A. Melton. 2008. Marked differences in differentiation propensity among human embryonic stem cell lines. *Nat. Biotechnol*. 26:313–315. doi:10.1038/nbt1383

Patel, S.R., J.H. Hartwig, and J.E. Italiano Jr. 2005. The biogenesis of platelets from megakaryocyte proplatelets. *J. Clin. Invest*. 115:3348–3354. doi:10.1172/JCI26891

Peerlinck, K., I. De Lepeleire, M. Goldberg, D. Farrell, J. Barrett, E. Hand, D. Panebianco, H. Deckmyn, J. Vermylen, and J. Arnout. 1993. MK-383 (L-700,462), a selective nonpeptide platelet glycoprotein IIb/IIIa antagonist, is active in man. *Circulation*. 88:1512–1517.

Raya, A., I. Rodríguez-Pizà, G. Guenechea, R. Vassena, S. Navarro, M.J. Barrero, A. Consiglio, M. Castellà, P. Río, E. Sleep, et al. 2009. Disease-corrected haematopoietic progenitors from Fanconi anaemia induced pluripotent stem cells. *Nature*. 460:53–59. doi:10.1038/nature08129

Rylski, M., J.J. Welch, Y.Y. Chen, D.L. Letting, J.A. Diehl, L.A. Chodosh, G.A. Blobel, and M.J. Weiss. 2003. GATA-1-mediated proliferation arrest during erythroid maturation. *Mol. Cell. Biol*. 23:5031–5042. doi:10.1128/MCB.23.14.5031-5042.2003

Schiffer, C.A. 2001. Diagnosis and management of refractoriness to platelet transfusion. *Blood Rev.* 15:175–180. doi:10.1054/blre.2001.0164

Schulze, H., and R.A. Shivdasani. 2005. Mechanisms of thrombopoiesis. *J. Thromb. Haemost.* 3:1717–1724. doi:10.1111/j.1538-7836.2005.01426.x

Shattil, S.J., J.A. Hoxie, M. Cunningham, and L.F. Brass. 1985. Changes in the platelet membrane glycoprotein IIb.IIIa complex during platelet activation. *J. Biol. Chem.* 260:11107–11114.

Takahashi, K., K. Tanabe, M. Ohnuki, M. Narita, T. Ichisaka, K. Tomoda, and S. Yamanaka. 2007. Induction of pluripotent stem cells from adult human fibroblasts by defined factors. *Cell.* 131:861–872. doi:10.1016/j.cell.2007.11.019

Takayama, N., H. Nishikii, J. Usui, H. Tsukui, A. Sawaguchi, T. Hiroyama, K. Eto, and H. Nakauchi. 2008. Generation of functional platelets from human embryonic stem cells in vitro via ES-sacs, VEGF-promoted structures that concentrate hematopoietic progenitors. *Blood.* 111:5298–5306. doi:10.1182/blood-2007-10-117622

Takeuchi, K., M. Satoh, H. Kuno, T. Yoshida, H. Kondo, and M. Takeuchi. 1998. Platelet-like particle formation in the human megakaryoblastic leukaemia cell lines, MEG-01 and MEG-01s. *Br. J. Haematol.* 100:436–444. doi:10.1046/j.1365-2141.1998.00576.x

Takizawa, H., S. Nishimura, N. Takayama, A. Oda, H. Nishikii, Y. Morita, S. Kakinuma, S. Yamazaki, S. Okamura, N. Tamura, et al. 2010. Lnk regulates integrin alphaIIbbeta3 outside-in signaling in mouse platelets, leading to stabilization of thrombus development in vivo. *J. Clin. Invest.* 120:179–190. doi:10.1172/JCI39503

Thompson, A., Y. Zhang, D. Kamen, C.W. Jackson, R.D. Cardiff, and K. Ravid. 1996a. Deregulated expression of c-myc in megakaryocytes of transgenic mice increases megakaryopoiesis and decreases polyploidization. *J. Biol. Chem.* 271:22976–22982. doi:10.1074/jbc.271.38.22976

Thompson, A., Z. Zhao, D. Ladd, J. Zimmet, and K. Ravid. 1996b. A new transgenic mouse model for the study of cell cycle control in megakaryocytes. *Stem Cells.* 14:181–187. doi:10.1002/stem.5530140723

Tomer, A. 2004. Human marrow megakaryocyte differentiation: multiparameter correlative analysis identifies von Willebrand factor as a sensitive and distinctive marker for early (2N and 4N) megakaryocytes. *Blood.* 104:2722–2727. doi:10.1182/blood-2004-02-0769

van der Meer, P.F., and R.N. Pietersz. 2005. Gamma irradiation does not affect 7-day storage of platelet concentrates. *Vox Sang.* 89:97–99. doi:10.1111/j.1423-0410.2005.00647.x

Vodyanik, M.A., J.A. Bork, J.A. Thomson, and I.I. Slukvin. 2005. Human embryonic stem cell-derived CD34+ cells: efficient production in the coculture with OP9 stromal cells and analysis of lymphohematopoietic potential. *Blood.* 105:617–626. doi:10.1182/blood-2004-04-1649

Vyas, P., K. Ault, C.W. Jackson, S.H. Orkin, and R.A. Shivdasani. 1999. Consequences of GATA-1 deficiency in megakaryocytes and platelets. *Blood.* 93:2867–2875.

Wang, L., L. Li, F. Shojaei, K. Levac, C. Cerdan, P. Menendez, T. Martin, A. Rouleau, and M. Bhatia. 2004. Endothelial and hematopoietic cell fate of human embryonic stem cells originates from primitive endothelium with hemangioblastic properties. *Immunity.* 21:31–41. doi:10.1016/j.immuni.2004.06.006

Webb, I.J., and K.C. Anderson. 1999. Risks, costs, and alternatives to platelet transfusions. *Leuk. Lymphoma.* 34:71–84.

Woll, P.S., B. Grzywacz, X. Tian, R.K. Marcus, D.A. Knorr, M.R. Verneris, and D.S. Kaufman. 2009. Human embryonic stem cells differentiate into a homogeneous population of natural killer cells with potent in vivo antitumor activity. *Blood.* 113:6094–6101. doi:10.1182/blood-2008-06-165225

Yokoyama, Y., T. Suzuki, M. Sakata-Yanagimoto, K. Kumano, K. Higashi, T. Takato, M. Kurokawa, S. Ogawa, and S. Chiba. 2009. Derivation of functional mature neutrophils from human embryonic stem cells. *Blood.* 113:6584–6592. doi:10.1182/blood-2008-06-160838

Yu, J., M.A. Vodyanik, K. Smuga-Otto, J. Antosiewicz-Bourget, J.L. Frane, S. Tian, J. Nie, G.A. Jonsdottir, V. Ruotti, R. Stewart, et al. 2007. Induced pluripotent stem cell lines derived from human somatic cells. *Science.* 318:1917–1920. doi:10.1126/science.1151526